Biochimica et Biophysica Acta 1840 (2014) 3277–3283

Contents lists available at ScienceDirect

Biochimica et Biophysica Acta

journal homepage: www.elsevier.com/locate/bbagen

Assembly of phagocyte NADPH oxidase: A concerted binding process?

Gilda Karimi [a], Chantal Houée Levin [a], Marie Claire Dagher [b], Laura Baciou [a], Tania Bizouarn [a,c,*]

[a] Laboratoire de Chimie Physique, Université Paris Sud, UMR8000, CNRS, Orsay F-91405, France
[b] Laboratoire TIMC-IMAG, Equipe TheREx, UMR5525, 38710 La Tronche, France
[c] Laboratoire de Chimie Physique, bat 350, Université Paris Sud, 91405 Orsay cedex, France

ARTICLE INFO

Article history:
Received 4 January 2014
Received in revised form 11 July 2014
Accepted 30 July 2014
Available online 7 August 2014

Keywords:
NADPH oxidase (Nox)
Protein translocation
Cell free system
Arachidonic acid activation
Neutrophil

ABSTRACT

Background: The phagocyte NADPH-oxidase is a multicomponent enzyme that generates superoxide anions. It comprises a membrane redox component flavocytochrome b_{558} and four cytosolic proteins ($p67^{phox}$, $p47^{phox}$, $p40^{phox}$ and Rac) that must assemble to produce an active system. In this work we focused on the spatio-temporal control of the activation process of phagocyte NADPH oxidase.
Methods: A wide range of techniques including fast kinetics with a stopped-flow apparatus and various combinations of the activating factors was used to test the order of assembly and the role of the $p47^{phox}$–$p67^{phox}$ complex.
Results: The data presented here are consistent with the absence of a catalytic role of the $p47^{phox}$–$p67^{phox}$ interacting state and support the idea of independent binding sites for the cytosolic proteins on the flavocytochrome b_{558} allowing random binding order. However, the formation of the active complex appears to involve a synergistic process of binding of the activated cytosolic subunits to cytochrome b_{558}. All partners should be in the vicinity for optimal assembly, a delay or the absence of one of the partners in this process seems to lead to a decrease in the efficiency of the catalytic core.
Conclusion and general significance: The activation and assembly of the NADPH oxidase components have to be achieved simultaneously for the formation of an efficient and optimal enzyme complex. This mechanism appears to be incompatible with continuous fast exchanges of the cytosolic proteins during the production of superoxide ion in the phagosome.

1. Introduction

Neutrophils are essential actors of the first line of defence in the fight against micro-organisms. In order to destroy the engulfed pathogens, they produce massive amounts of reactive oxygen species (ROS) on their surface. This ROS production is generated from the superoxide ions formed by a reduction of molecular oxygen with NADPH as an electron donor, catalysed by the NADPH oxidase, a multi-component membrane enzyme complex. This complex consists of six proteins, four cytosolic proteins, namely $p40^{phox}$, $p47^{phox}$, $p67^{phox}$ and Rac and two membrane proteins, $gp91^{phox}$ (also called Nox2) and $p22^{phox}$, that form the flavocytochrome b_{558} (cyt b_{558}). Because of the noxious properties of the ROS, their production has to be very finely controlled. This is achieved by a precise spatial and temporal regulation [1–3]. In the absence of pathogens, the neutrophils adopt a resting state in which the NADPH oxidase enzyme is inactive through a separate localisation in the cell of the soluble and the membrane partners. The first ones are maintained in the cytosol and the last ones in specific granules and plasma membrane. All these subunits associate in a stimulus-dependent manner to form the active state of the enzyme. Binding studies between the different soluble proteins performed in vitro suggested that three of the cytosolic proteins are preassembled as a trimer $p40^{phox}$–$p47^{phox}$–$p67^{phox}$ [4–6]. This heterotrimer could be the predominant form that, during the activation process, goes to the membrane to interact with cyt b_{558} since $p67^{phox}$ is unable to translocate to the membrane without $p47^{phox}$ [7–9]. Rac, the fourth cytosolic protein participating in the formation of the NADPH oxidase complex would translocate on its own to the membrane [10,11]. The activation process starts by the binding on receptors of soluble or particulate stimuli that promotes the phosphorylation of most of the components of the NADPH oxidase, $p47^{phox}$ being the most affected by this event. Actually, phosphorylation of $p47^{phox}$ produces conformational changes leading to the exposure of two SH3 motifs, a proline-rich region, a PX domain and an auto-inhibitory domain [12–15]. This structural change leads to interactions of $p47^{phox}$ with both cyt b_{558} and phosphoinositides present in the phagosomal membrane. Experiments done with $p67^{phox}$-N terminal segment (1–242) suggested that there was a need to unmask some region of $p67^{phox}$ to render it fully active [13]. However there is no strong evidence that these changes of $p67^{phox}$ conformation are induced by

Abbreviations: AA, arachidonic acid; FRET, Forster resonance energy transfer; GST, glutathione S transferase; ITC, isothermal titration calorimetry; MF, membrane fraction of human neutrophils; Nox, NADPH oxidase; Phox, phagocyte oxidase; PBS, phosphate buffer saline; PMSF, phenylmethylsulfonyl fluoride; PX domain, phagocyte oxidase domain; ROS, reactive oxygen species; SH3, Src homology 3

* Corresponding author. Tel.: +33 1 69153016.
E-mail address: tania.bizouarn@u-psud.fr (T. Bizouarn).

http://dx.doi.org/10.1016/j.bbagen.2014.07.022
0304-4165/

phosphorylation and a recent work of El Benna's group showed that p67^{phox} is constitutively partially phosphorylated [16]. It is therefore unclear whether modifications of this protein conformation occur during the activation of the neutrophil.

The role of each protein is also very different. It is well established that cyt b_{558} contains all the redox machinery to support the superoxide anion production, namely the binding sites for NADPH, FAD and two hemes. While p47^{phox} is described as the adaptor for the translocation to the cyt b_{558}, it seems to have a weak role in the activity per se [1–3]. Recent studies suggest that it may even stay only a short time bound on the cyt b_{558} at the beginning of the activation process and disassemble before the end of the superoxide production [17]. On the other hand, p67^{phox} has a crucial role in the initiation and maintenance of the activation of the cyt b_{558} and therefore p67^{phox} is called the activator protein [1–3,18].

The aim of our study is to better understand the mechanism of assembly and activation of the NADPH oxidase complex and more specifically the interaction between p47^{phox} and p67^{phox}. Despite all published works about the assembly it is still not clear whether it is an ordered or random process. We studied in particular the relationship between the duration of assembly and the resulting specific activity of the assembled enzyme. In addition we addressed the stability of the p47^{phox}–p67^{phox} complex by measuring its dissociation constant in the resting and active states. The understanding of the system has been greatly assisted by the use of the cell free system, which helps understand the role of each component independently from the others [19]. Moreover it is a unique way for the acquisition of precise kinetic data. We used an array of techniques including fast kinetics with a stopped-flow apparatus that allows recording of the superoxide production a few milliseconds after mixing the components of the cell-free system. It is well known that in the cell free system, the presence of arachidonic acid allows some components to adopt the active form [12,13,19]. Thus the role of this molecule in the assembly has been also considered.

2. Materials and methods

2.1. Materials

Competent BL21(DE3) cells were purchased from Life Technologies, France. Chromatographies were carried out using SP-Sepharose, Q-Sepharose, Glutathione HP-Sepharose, and Ni-Sepharose resins from GE Healthcare, France. Arachidonic acid and equine heart cytochrome *c* were from Sigma-Aldrich, France and NADPH from ACROS, France.

2.2. Protein and plasmid preparations

The plasmids coding for the human cytosolic proteins, pET15b-Hisp67^{phox}, pET15b-Hisp47^{phox} and pGEX2T-GSTRac1Q61L were provided by Dr. M.C. Dagher, Grenoble, France; and the plasmid pGEX6P-p47^{phox}-ΔCter (aa 1–342) was provided by Pr. F. Fieschi, Grenoble, France [20]. The GTP like form of Rac1 obtained by the mutation Q61L was used in all the experiments presented in this paper. Rac1Q61L was renamed Rac for simplification. All the plasmids were checked for their sequence and used for transformation of *Escherichia coli* BL21(DE3). Purification of p47^{phox}, p67^{phox} and Rac1Q61L was performed mainly as previously described [21]. Briefly, after a first step through an ion exchange column, the fusion protein was purified by affinity chromatography on Ni-Sepharose or Glutathione-Sepharose. The protein was then dialysed overnight against a phosphate buffer (30 mM sodium phosphate, pH 7.5, 100 mM NaCl) and stored at −80 °C. The concentration was established using BCA assay (Pierce) and by the absorbance at 280 nm using a NanoDrop2000 spectrophotometer (Thermo Scientific, France), the extinction coefficient being estimated from the amino acid sequences (Expasy, SIB Bioinformatics Resources Portal). The purity was controlled by SDS gel (10% Bis–Tris Nupage, Invitrogen) using Coomassie Blue reagent and quantified by the ImageJ software. SDS gels in the presence and the absence of β-mercaptoethanol allowed distinguishing between monomeric and dimeric forms of proteins.

2.3. Gel filtration chromatography

The gel exclusion chromatography was performed on a Superdex 75 Hiload 16/60 column (GE Healthcare, France) equilibrated with buffer (30 mM sodium phosphate, pH 7.5, 150 mM NaCl, 2 mM dithiothreitol and 1 mM PMSF). The volume of the injected solution was 500 μl and contained an equimolar concentration of proteins ranging between 20 and 25 μM when a mix of proteins was used. The column was run at 4 °C with a flow rate of 0.5 ml/min. The sample was eluted with an equilibration buffer. The MW protein standard mix (MWND-500, Sigma) was used to calibrate the column: proteins of 132, 66, 45 and 29 kDa were eluted at 47–48 ml, 53–54 ml 59–60 ml and 65–66 ml respectively.

2.4. Neutrophil membrane preparation

The neutrophils were purified from the human blood as described in Ref. [22]. Briefly, 500 ml of blood was sedimented in 2% dextran solution, then the neutrophils were separated from lymphocytes by centrifugation on Ficoll solution and the red cells were removed after their lysis by centrifugation. After sonication, neutrophil membranes and cytosol were separated by ultra-centrifugation for 1 h at 200000 ×*g*. The membrane fraction was re-solubilised in a lysis buffer (20 mM sodium phosphate, pH 7.4, 340 mM sucrose, 7 mM $MgSO_4$, 0.2 mM leupeptin and 1 mM PMSF) by a brief sonication and stored at −80 °C in aliquots. The differential spectrum of reduced minus oxidized cytochrome b_{558} was recorded from each preparation and the amount of heme was quantified using an extinction coefficient of 200 $mM^{-1}\cdot cm^{-1}$ at the Soret band (427 *minus* 411 nm).

2.5. Measurement of the superoxide production in cell-free assays

Unless indicated otherwise, the membrane fraction (2.5 nM cyt b_{558}), p67^{phox} (250 nM), p47^{phox} (200 nM) and Rac (500 nM) were incubated in the presence of 26 μM arachidonic acid (AA) in 500 μl phosphate buffer saline supplemented with 10 mM $MgSO_4$ for 5 min at room temperature (25 °C). The production was initiated by the addition of NADPH (250 μM) and the rate of $O_2^{\bullet-}$ was quantified by cytochrome *c* (50 μM) reduction. The rate was measured at 550 nm in a Thermo Evolution 500 spectrophotometer, with an extinction coefficient ε of 21000 M^{-1} cm^{-1} (reduced *minus* oxidized). In the absence of an incubation period, a lag appears before obtaining the full superoxide production rate, which is assumed to reflect a phase of assembly of the Nox complex. For the study of this lag the following protocol was used. The proteins and arachidonic acid were added, as quickly as possible, to a final volume of 500 μl of PBS buffer supplemented with 10 mM $MgSO_4$ in the order indicated in the figure legend and superoxide anion production was measured immediately after the last component was added.

2.6. Determination of enzymatic parameters

The enzymatic parameters, EC_{50} and $V_{max,}$ were determined by non-linear least square fitting of the curves of superoxide rate of production vs. component concentration using the following expression.

$$V = \frac{V_{max}[P]}{EC50 + [P]} \quad (1)$$

where [P] is the concentration of the considered protein (p67^{phox}, p47^{phox} or Rac).

2.7. Stopped flow measurements

The experiments were done with a SX20 instrument (Applied Photophysics, U.K.) using the photodiode array setup. Absorbance at 550 nm was measured with a slit width of 3 mm at the monochromator, at 25 °C, for 3 min. The mixture of each syringe was prepared so that a 5 min incubation was maintained before starting the measurement. In some cases, the superoxide production was also measured after longer incubation periods (8 or 11 min). The concentrations of the components present in the syringes were: membrane fraction (5 nM of cyt b_{558}), $p67^{phox}$ (500 nM), $p47^{phox}$ (400 nM), Rac (1 μM), arachidonic acid (52 μM), NADPH (500 μM) and cyt *c* (100 μM), in PBS buffer supplemented with 10 mM $MgSO_4$ leading to concentrations in the measurement cuvette identical to those described for the spectrophotometer. The composition of the solution loaded in the two syringes is indicated in the table legend.

2.8. K_d measurements with a Surface Plasmon Resonance system

Data were recorded on a Biacore 2000 Surface Plasmon Resonance system using a Ni-NTA sensor chip. The experiments were performed mainly as recommended by the manufacturer. The running buffer used was 10 mM Hepes, 250 mM NaCl, 50 μM EDTA, and 0.005% surfactant P20, pH = 7.4. While 10 μl of His-$p67^{phox}$ at a concentration of 30 nM was fixed on the surface, a titration with $p47^{phox}$ was done with the following concentrations: 100 nM, 50 nM, 25 nM, 12.5 nM and 6.25 nM. The K_d value was obtained by using the Biacore 2000 software and determined by the equation corresponding to "one site, two states" model as described in the Supplementary material.

3. Results

3.1. Assessing the $p47^{phox}$–$p67^{phox}$ interaction in the resting state

In the resting state of neutrophils, $p67^{phox}$ and $p47^{phox}$ are believed to be able to interact to form a heterodimer [5,23,24]. It is of interest to determine to what extent these proteins interact in their inactive states. Therefore, we investigated several approaches in order to estimate the dissociation constant between these two proteins in solution. It is well established that $p67^{phox}$ and $p47^{phox}$ interact through two domains situated in their C terminal parts [24,25]. The deletion of this region (from amino acid 343 to 390) in $p47^{phox}$ prevents these two proteins to dimerize [5]. Thus the protein $p47^{phox}$ΔCter (1–342) was used as negative control.

A qualitative analysis was first performed using size exclusion chromatography associated to SDS gel analyses (Fig. 1). This method was used for $p67^{phox}$, $p47^{phox}$ or $p47^{phox}$ΔCter alone, then for a mixture of $p67^{phox}$ with either $p47^{phox}$ or $p47^{phox}$ΔCter (Fig. 1). The chromatography profiles of each individual protein ($p67^{phox}$, $p47^{phox}$ or $p47^{phox}$ΔCter) gave two peaks (Fig. 1A and B, dashed lines), a small one corresponding to a dimeric form and a large one corresponding to the monomeric form of the protein. The monomeric and dimeric forms were confirmed by the migration of the proteins on SDS gels in reduced and non-reduced conditions (data not shown). The elution profile of a mix of two proteins gave three peaks (Fig. 1A and B, continuous lines), which could be attributed from SDS gels. The $p67^{phox}$ protein was identified mainly in peaks 1 and 2. In peak 3, only the monomer $p47^{phox}$ or $p47^{phox}$ΔCter was present. In peak 1, $p47^{phox}$ was present together with $p67^{phox}$ indicating the formation of a $p67^{phox}$–$p47^{phox}$ heterodimer (120–140 kDa). As expected, when the same procedure was performed with $p47^{phox}$ΔCter instead of $p47^{phox}$, $p47^{phox}$ΔCter was not detected in peak 1. Despite a high affinity (see below and Table 1), a rather small proportion of heterodimer was observed with this technique. This could be due to a dissociation of the complex during the elution since the heterodimer is not anymore in equilibrium in the column. It may also reflect conformational heterogeneity that enables proteins to form heterodimers. However, our data clearly show the presence of the $p67^{phox}$–$p47^{phox}$ heterodimer in the resting state in the solution.

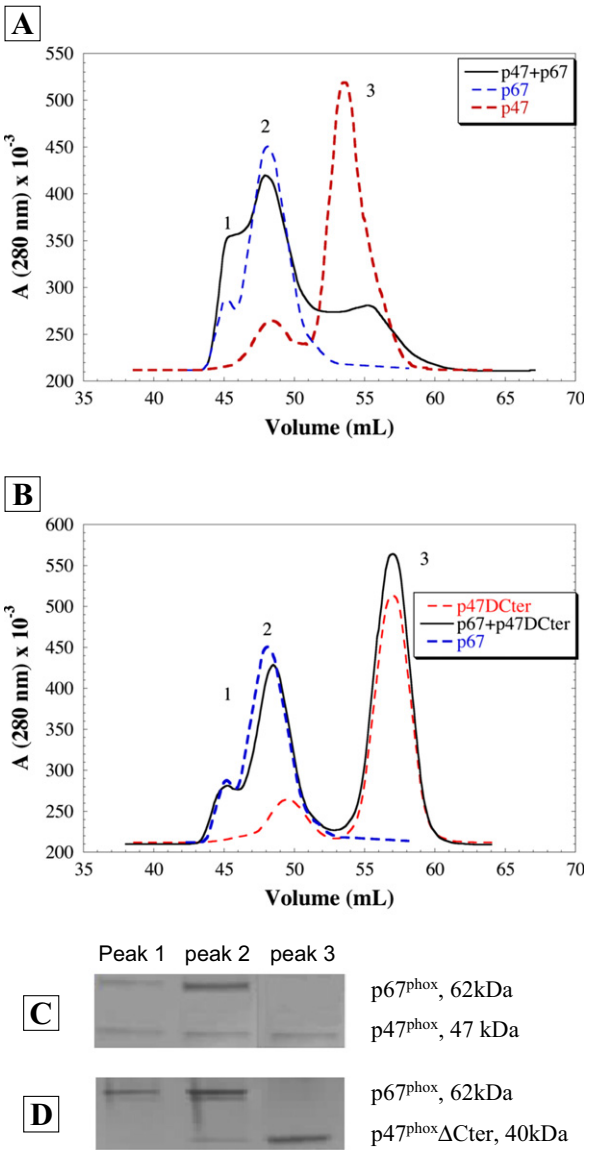

Fig. 1. Identification of the $p47^{phox}$–$p67^{phox}$ dimer formation by exclusion chromatography on a Superdex 75 column. A. Exclusion chromatography profile of a) an equimolar mix of $p67^{phox}$ and $p47^{phox}$ (continuous black line); b) $p47^{phox}$ (dashed red line); and c) $p67^{phox}$ (dashed blue line); B. Exclusion chromatography profile of a) an equimolar mix of $p67^{phox}$ and $p47^{phox}$ΔCter (aa 1–342) (continuous black line); b) $p47^{phox}$ΔCter (dashed red line); and c) $p67^{phox}$ (dashed blue line); and the positions of peaks 1, 2 and 3 are indicated. C. SDS-PAGE gel of the fractions 45, 47, and 55 from the elution of equimolar mix of $p67^{phox}$ and $p47^{phox}$; D. SDS-PAGE gel of the fractions 45, 48, and 57 from the elution of equimolar mix of $p67^{phox}$ and $p47^{phox}$ΔCter. For the conditions see the Materials and methods. These experiments have been performed with two different protein purification preparations and gave the same results.

Table 1
K_d values for the $p67^{phox}$–$p47^{phox}$ couple obtained by different methods. The binding curves obtained by Surface Plasmon Resonance and the model used for the K_d measurement are shown in the Supplementary materials (Figure S1).

Method	K_d (nM)	Reference
Surface Plasmon Resonance	4 ± 0.3	This work
Intrinsic fluorescence	32	[27]
ITC	20	[5]

In order to obtain more quantitative data, experiments attempting to measure the K_d value between $p47^{phox}$ and $p67^{phox}$, were performed (Table 1). However, we would like to emphasise that many methods including FRET and intrinsic tryptophan fluorescence changes, ITC, were tested, and led to unsatisfactory results due to the fragility, the high flexibility of these proteins and their high propensity to form aggregates. We mention here only the best result we have obtained by plasmon resonance. The K_d value that could be determined was compared to those described in the literature. Table 1 underlines that all methods converge to a low K_d value ranging between 4 and 30 nM, i.e. a high affinity of both proteins for each other.

3.2. Assessing the $p47^{phox}$–$p67^{phox}$ interaction in the active state

Arachidonic acid is a well-known activator molecule of the NADPH oxidase complex. It is proposed to target and activate the soluble $p67^{phox}$ and $p47^{phox}$ proteins. The same experiments as above were performed in the presence of this activator to identify if the interaction between both proteins was affected. Thus a mixture of $p67^{phox}$ and $p47^{phox}$ preincubated with 200 μM of arachidonic acid was analysed by size exclusion chromatography column used previously. Surprisingly, the same elution profile was obtained in the absence of the activator molecule (data not shown). The other techniques did not give any exploitable result, since AA interferes with the signals. This result suggests that arachidonic acid does not impact the interaction equilibrium of the $p67^{phox}$–$p47^{phox}$ dimer.

3.3. Assembly of the complex in a cell free system

We further questioned the affinities of each cytosolic protein for the activated complex. To that purpose we followed the assembly of the complex through its capacity to produce superoxide with a variable amount of one of the cytosolic proteins. The rate of the superoxide production for varying amounts of human His-tagged $p67^{phox}$, all other concentrations being maintained constant, is illustrated in Fig. 2. The protein concentration dependence could be fitted using a Michaelis–Menten like equation (see Materials and methods). Similar curves were obtained for the other cytosolic proteins. Table 2 shows the EC_{50} and V_{max} values obtained by fitting each curve by Eq. (1).

These values determined for $p47^{phox}$, $p67^{phox}$ or Rac are very different: $EC_{50}(p47) < EC_{50}(p67) \ll EC_{50}(Rac)$. Rac has a significantly lower affinity than the other cytosolic proteins for the complex with an EC_{50} value of about 5- and 20-fold higher than the EC_{50} values determined for $p67^{phox}$ and $p47^{phox}$, respectively. In contrast to an in vivo situation, Rac produced in *E. coli* is not prenylated which might decrease its affinity for the membrane and thus probably for cyt b_{558} and RacQ61L used here does not require any preloading with GTP to be active. In the absence of $p47^{phox}$, the $p67^{phox}$ protein can bind to the membrane fraction, albeit with a ten times higher EC_{50} and lower V_{max} values. Conversely as long as the $p47^{phox}$ concentration was well above its EC_{50}, i.e. over 50 nM, the rate did not vary with an increasing concentration of $p47^{phox}$ indicating that there is no competition between the two proteins for their binding to the complex (Fig. 3). Surprisingly, the absence of the interacting region with $p67^{phox}$ in the truncated $p47^{phox}$ protein (denoted as p47ΔCter in Table 2) had no effect on this EC_{50} (39 ± 6 nM), compared to the EC_{50} value of $p67^{phox}$ (30 ± 4 nM) in the presence of full $p47^{phox}$. Only a slight decrease in the V_{max} value was noticed.

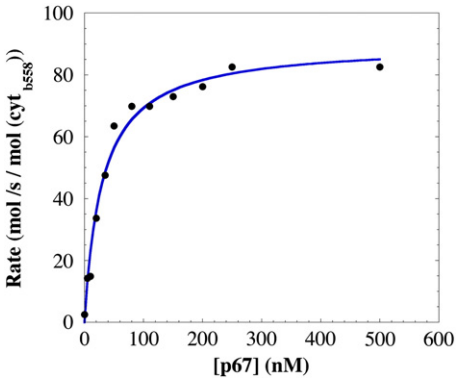

Fig. 2. Dependence of the NADPH oxidase activity as a function of $p67^{phox}$ concentration. The superoxide formation rate was measured by spectrophotometry as indicated in the Materials and methods. In addition to $p67^{phox}$, the proteins present were membrane fraction of human neutrophils (MF) ([cyt b_{558}] = 2.5 nM), $p47^{phox}$ (200 nM) and Rac (500 nM). The fit corresponds to values of EC_{50} and V_{max} of 30.2 ± 3.9 nM and 90.1 ± 4 mol of superoxide/s/mol of cyt b_{558} respectively.

Table 2
Kinetic parameters for the recombinant cytosolic proteins obtained using the Michaelis–Menten like equation. All concentrations of the proteins except those used for titration can be found in the Materials and methods. The results are given as percent of activity compared to the 100% activity of the control experiment realised on the same day ($p67^{phox}$, $p47^{phox}$, Rac) corresponding to 80–100 mol $O_2^{\bullet-}$/s/mol of cyt b_{558}. These experiments were performed in duplicate with a variation of 5% between EC_{50} and V_{max} values.

Protein used for the titration	Other cytosolic s.u. present	EC_{50} (nM)	V_{max} (%)
$p67^{phox}$	p47 + Rac	30 ± 4	100
$p67^{phox}$	Rac	257 ± 112	32 ± 6
$p47^{phox}$	p67 + Rac	7.7 ± 3.1	96 ± 5
Rac	p47 + p67	152 ± 52	116 ± 11
$p67^{phox}$	p47ΔCter + Rac	39 ± 6	80 ± 3

3.4. Deciphering the sequence of the assembly

It is well known that, if no incubation takes place before the measurement of activity, in other words if NADPH is added immediately after AA, a lag of around 1 min is observed on kinetics before a maximal rate of superoxide production is reached (Fig. 4 and Ref. [26]). In a previous study we have shown that the process leading to the assembly, which takes place during the incubation period, involves at least two major phases. During the first phase, the proteins are more sensitive to ROS than during the second one [27]. It was of interest to see the evolution of the lag (the first phase) and the rate (the second phase) as a function of the incubation period. As shown in Fig. 4, the curves exhibit an initial curvature characteristic of a non-steady state situation. The curvature disappears after 1 min of the incubation period i.e. the time between the addition of AA and of NADPH (Fig. 4A). This is associated with an increase in the initial rate of superoxide production, the optimum being usually reached after 5 min of incubation.

To grasp information about the sequences and the duration of these steps, we first performed experiments by a classical spectrophotometry. Fig. 4B shows the kinetic curves without the incubation period with different sequences of the addition of the NADPH oxidase complex components relative to the AA addition. We noticed that the rank of arachidonic acid addition (last, last but one or second) modulates the lag period and the rate. This indicates that the first phase of assembly (around 1 min) is controlled by arachidonic acid interactions and that the edification of the active complex requires the presence of all the proteins at the starting point of the AA activation to be optimum. The assembly leading to the highest superoxide production was obtained when all the components were first pre-mixed before AA was added (#1) while when the membrane fraction (#6) or when the three cytosolic proteins (#5) were added after AA, the mixtures led to lower rates. The second phase corresponding to an increase of the rate value that lasts 5–8 min seems to reflect an adjustment of the protein interactions within the complex.

To further study the impact of the order of addition of the proteins and their binding rates on cyt b_{558}, we measured the superoxide production by using a stopped flow apparatus coupled to absorption

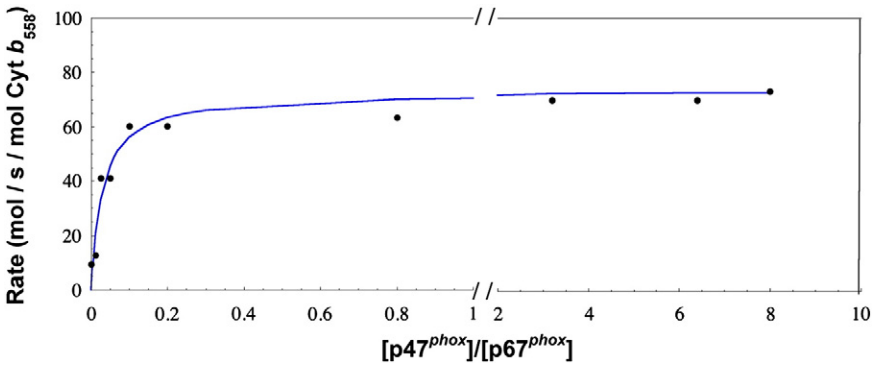

Fig. 3. NADPH oxidase activity as a function of the [p47^{phox}]/[p67^{phox}] ratio. The concentration of p67^{phox} and Rac were 250 nM, and 500 nM respectively. The concentration of p47^{phox} was varied from 3 nM to 2 μM. The rate of superoxide production was measured as described in the Materials and methods. This experiment was done in triplicate.

detection (Table 3). This methodology allows mixing of solutions within the millisecond time scale. The final content of the detection cell during the activity measurement was identical in all ten configurations, but the content of the syringes was different (Table 3). The substrate of the reaction NADPH and cyt *c* was always added in syringe 2. In agreement with the results in Fig. 4, we observed that, depending on the situation, the initial rates were very different; however no lag was seen (data not shown), and the kinetics were linear from the start. It is likely that the first phase triggered by AA is not detectable by this method because of the time required for syringe preparation.

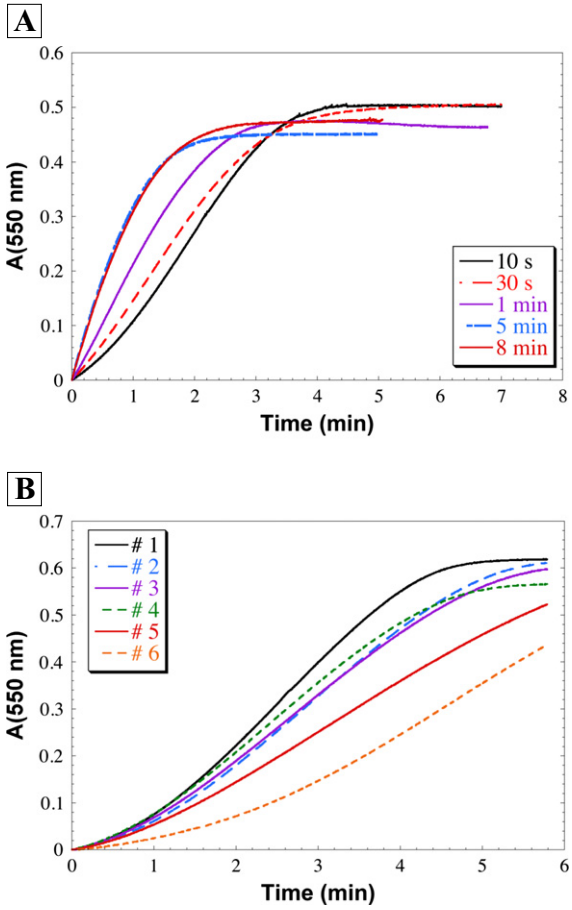

Fig. 4. Time course of superoxide anion production generated by the NADPH oxidase complex formed by varying the order of addition of the components. (A) The order of addition of the components in the cuvette was MF, p67, p47, Rac, then AA with a variable incubation period before the addition of NADPH of 10 s (continuous black line); 30 s (dashed red line), 1 min (violet line) ,5 min (dashed blue line) and 8 min (continuous red line). (B) No incubation was done in (#1 to #6). The order of addition for the components were (#1), MF, p67, p47, Rac, then AA; (#2) MF, p47, Rac, AA then p67; (#3) MF, p67, p47, AA then Rac; (#4) MF, p67, Rac, AA then p47; (#5) MF, AA, p67, p47 then Rac; and (#6) p67, p47, Rac, AA then MF. The "zero" time corresponds to the addition of NADPH. This experiment was reproduced with three different neutrophil membrane preparations.

The highest initial activities could be reached in situations #2 (where all the proteins were incubated with AA) and #1 (where only MF was incubated with AA). In situation #2, the mixture corresponds to the classical cell-free system where all components are mixed together. Obviously, the initial activity was stable and even tended to increase with longer incubation time. In contrast to situation #2, a strong decrease in the superoxide production was observed in situation #1 with longer incubation time. A similar decrease of activity as function of the incubation period was also observed from the first minute of incubation with a classical spectrophotometer. This led us to conclude that the presence of all components during the activation is a prerequisite for an efficient superoxide production.

The effect was drastic when the membrane fraction (#10) or AA (#11) was provided in the second syringe, thus it had no previous contact with the other partners. Although the result in configuration #11 was obvious since no activation was possible, the former can be attributed to a requirement of the MF to incubate with AA. A low NADPH oxidase activity when AA was added before MF had already been described in Fig. 4 (#7).

We observed that lower activities were detected whenever one or two partners were not in contact with AA, especially if this partner is

Table 3
Superoxide anion production rate measured using stopped flow equipment. The superoxide production rate was measured by following cytochrome *c* reduction at 550 nm. The contents of the two syringes are indicated. The rates were measured immediately after mixing the content of syringe 1 and syringe 2. Before mixing, the components were incubated separately in their respective syringes for the following times: 5, 8 and 11 min. This experiment has been carried out with three different MF preparations. From each curve, the rate was determined with a standard deviation close to 1%, however a 5% variation for each case relative to the optimal value was observed between MF preparations.

#	Content of syringe 1	Content of syringe 2	Initial rate (mol $O_2^{\bullet-}$/s/mol of cyt b_{558})		
			Incubation time		
			5 min	8 min	11 min
1	MF AA	p47 p67 Rac NADPH cyt c	127	63.7	9.19
2	MF AA p47 p67 Rac	NADPH cyt c	67.8	122	125
3	MF AA p47	p67 Rac NADPH cyt c	22.8	16.5	13.3
4	MF AA p47	NADPH cyt c	3.0		
5	MF AA p67	p47 Rac NADPH cyt c	6.9		
6	MF AA Rac	p67 p47 NADPH cyt c	5.1		
7	MF AA p67 p47	Rac NADPH cyt c	26.0		
8	MF AA p67 Rac	p47 NADPH cyt c	25.4	34.2	38
9	MF AA p47 Rac	p67 NADPH cyt c	8.2		
10	p47 p67 Rac AA	MF NADPH cyt c	7.0	6.5	7.0
11	MF p47 p67 Rac	AA NADPH cyt c	8.2		
12	MF AA	NADPH cyt c	3.0		

p67^{phox} (#6 and #9). When p67^{phox} and Rac or p67^{phox} and p47^{phox} were incubated with MF (situations #7 and #8), the activity reached values ranging between 20 and 35% of the value of #2. Again, in situation #3, when MF was incubated with p47^{phox}, we observed 20% of the maximum activity. In this context, a pre-complex (syringe 1) was probably formed by the membrane fraction and the proteins activated by AA. The partners added later on were able to interact with the pre-complex but were unable to form the optimal state of the enzyme. In conclusion, these experiments revealed states of the complex where the binding of the subunits is impaired, which leads to a superoxide production activity of about 20–35% of the maximal one. Therefore it is likely that both Rac and p47^{phox} participate in the stabilization of the complex between cyt b_{558} and p67^{phox}.

4. Discussion

In cells, the NADPH oxidase activity is very dependent on signalling pathways, thus the comparison of results obtained in vitro and in vivo may not be straightforward. However, the study of enzymes in cell free systems can give detailed information on each step of assembly and on the reaction that could not be obtained in vivo.

In the resting state of neutrophils, the three cytosolic proteins p40^{phox}, p47^{phox}, and p67^{phox} have been proposed to form a trimer. Rac is separated and is associated with GDP-Dissociation Inhibitor protein. It is well accepted that upon activation, the cytosolic proteins p47^{phox}, p67^{phox} and Rac assemble to flavocytochrome b_{558} in a 1:1:1:1 complex [1–3]. The activation of the NADPH oxidase is triggered either by a stimulus (in vivo) or by an amphiphile molecule (in vitro) and involves conformational changes in these subunits and their translocation to flavocytochrome b_{558}. In this paper our aim was to shed some light on the different steps of the assembly.

4.1. Two different binding sites of p47^{phox} and p67^{phox} on the flavocytochrome b_{558}

Comparison with previous data is difficult because of the discrepancy in the procedures used. As shown in this paper, the incubation period is critical. Different protocols that affect the EC_{50} values are currently used: mixing of very concentrated proteins solutions, followed by dilution [19,28]; the use of purified and relipidated cytochrome b_{558} [19,29,30]. For example, if the complex does not dissociate after dilution, the EC_{50} should be calculated from the concentration used during the incubation period and not during the activity measurement.

If we assume that binding of a protein P to the catalytic core cyt b_{558}, is required for activity and that it remains bound during catalysis, then the EC_{50} of protein P can be assimilated to its dissociation constant K_d with respect to cyt b_{558}. An additional factor, inherent to the activation of Nox that could overestimate the K_d values is that all the proteins are not necessarily in the activated state, while only this state should be taken into consideration for the calculation. Similar EC_{50} for the three cytosolic proteins were obtained when they were combined with bovine MF and human MF even if they were activated with very different ranges of AA (data not shown). Therefore, in these experimental conditions the activation of cytosolic proteins is not a limiting factor of the assembly process.

Our results are in agreement with the hypothesis of separate binding sites for p47^{phox} and p67^{phox} on the cytochrome [1,28,31]. Indeed: i) in the absence of p47^{phox}, p67^{phox} is able to participate in an active complex (this paper and Refs. [30] and [32]; ii) deletion of the C-terminal region of p47^{phox}, which is involved in the p47^{phox}–p67^{phox} complex does not prevent the binding of p67^{phox} to cyt b_{558}; and iii) the determined EC_{50} values are different for each cytosolic protein. If one makes the hypothesis that both p47^{phox} and p67^{phox} translocate together to the cyt b_{558} as it occurs in vivo, the different EC_{50} values measured (8 nM vs. 30 nM for p47^{phox} and p67^{phox}, respectively) imply that their dissociation rate constants from cyt b_{558} are different. A similar reasoning about Rac binding leads to an equivalent conclusion. Our proposal, based on kinetics data, of three different sites on the flavocytochrome b_{558} is in agreement with the presence of three interacting regions that have been described from biochemical and structural approaches: p67^{phox} interacting with the cytosolic C terminal part of gp91^{phox} [31], the SH3 domains of p47^{phox} with the proline rich region of p22^{phox} [20] and the insert region (124–135) of Rac with cyt b_{558}. This last interaction however is still controversial [33]. Finally, it has been seen by atomic force microscopy technique that p67^{phox} and p47^{phox} could bind independently [34].

Although their binding sites on cyt b_{558} are different, our data indicate that the binding of one of the cytosolic proteins to cyt b_{558} induces conformational changes of the latter, therefore indirectly increasing the affinity of the other cytosolic proteins.

4.2. The dimerization of p67^{phox} with p47^{phox} is not necessary for activity

The interacting region between p47^{phox} and p67^{phox} has been clearly identified at their C-terminal parts [24]. It has been shown that deletion of the p47^{phox} end decreased considerably the affinity between p47^{phox} and p67^{phox} [5,24,30]. Our results show that this interaction does not significantly affect their affinity for cyt b_{558}, since the deletion of p47^{phox} C-ter had no substantial effect on the EC_{50} of p67^{phox} (this paper and Ref. [13]). The minor effect on V_{max} suggests that the interacting region is not implicated in the activation process that leads to active forms of p47^{phox} and p67^{phox}. Conversely, the activation by AA of these two proteins does not significantly affect their affinity for each other. Moreover, it is conceivable that their binding on cyt b_{558} induces a separation between these two components. This proposal is based on the fact that these C-terminal parts have no role in activity and that the dissociation rate of p47^{phox} and p67^{phox} from cyt b_{558} is different. The disruption of this interaction had also been suggested in cells using fluorescently tagged C-terminal fragment of p47^{phox} [35]. This scheme is in accordance with the data showing that in vivo p47^{phox} leaves permanently the complex during the superoxide production [17]. The role of this tail to tail interaction would be mainly to facilitate translocation of p67^{phox} to the membrane.

4.3. What is happening during the lag period?

Our kinetic data performed on classical spectrophotometer show that all the proteins must be activated at the same time, a delay of around 10 s only (the time between the addition of two proteins) leading to a decrease of the activity. The experiments performed on the stopped flow apparatus (Table 3) show that the activity and the stability of the complex are highly dependent on the composition of the mixture present in the syringes. For example when two cytosolic proteins were not incubated in the presence of the membrane fraction, a fully active NADPH oxidase complex was not formed. Some conclusions can be highlighted: i) the three cytosolic proteins should be in contact with cyt b_{558} at the same time for the formation of an efficient and stable complex, and ii) the binding of these proteins to the membrane fraction seems to be fast since no lag period was observed. This set of data also suggests that a protein missing during the incubation period has great difficulties to assemble to the complex already formed. These observations indicate that the activation of the three cytosolic proteins and their binding to cyt b_{558} have to be simultaneous for an optimal complex enzyme to form. If this phenomenon occurs in cells, it means that the rate of the cytosolic protein association on cyt b_{558} may account for the regulation of the superoxide production rate. Moreover, it suggests that the cytosolic partners do not dissociate and associate during the superoxide ion production. Therefore there would be no need for continuous phosphorylation and dephosphorylation of p47^{phox} during phagocytosis [36]. This underlines the importance of the p40^{phox}–p47^{phox}–p67^{phox} trimer to bring simultaneously the cytosolic partners onto cyt b_{558}.

The effect of the composition on the stability of the complex was nicely described by Miyano et al. [19] where they have shown that the flavocytochrome b_{558} was unstable in its active form and that the stability of the enzyme was increased by the presence of the three cytosolic proteins $p47^{phox}$, $p67^{phox}$ and Rac and greatly enhanced by the fusion of p67N–p47 in presence of the Rac Q61L mutant. Our data and Miyano's confirm in vitro and extend prior studies of the NADPH oxidase assembly in intact cells. Indeed, our statement on the importance of complex stability completes the description of Grinstein [37] and that of Dinauer's group [38] who describes the role of phosphatidylserine distribution during the maturation of phagosome in protein targeting and the role of $p40^{phox}$ in the stability of the enzyme. The regulation mechanisms described in this paper may be related to the variation observed with different signalling activation pathways.

In conclusion, the data presented here are consistent with different binding sites on flavocytochrome b_{558} for the three cytosolic proteins $p47^{phox}$, $p67^{phox}$ and Rac. The order of binding is random for $p47^{phox}$, $p67^{phox}$ and probably also for Rac. The activation and assembly have to be achieved concomitantly for the formation of an efficient and optimal complex. The interaction existing in the cytosol between $p47^{phox}$ and $p67^{phox}$ has a minor catalytic role, in opposite to the interaction between Rac and $p67^{phox}$ [39,40], but it is an important means to bring the cytosolic proteins together, simultaneously, on the cyt b_{558}. Our data are in agreement with and extend prior studies of the NADPH oxidase based on the cell-free assay or intact cells. However, it is clear that the situation is different in vivo since all the subunits of the complex are essential for assembly and activation.

Acknowledgements

We are indebted to Prof. F. Fieschi for the plasmids, to Prof. O. Nüsse for helpful discussions and F. Lederer for her help in the purification of MF. We thank Dr. N. Thielens for help with the Biacore technology. The ANR-2010-BLAN-1536-01 and the COST action CM1201 (Biomimetic Radical Chemistry) are acknowledged for financial support.

Appendix A. Supplementary data

Supplementary data to this article can be found online at http://dx.doi.org/10.1016/j.bbagen.2014.07.022.

References

[1] H. Sumimoto, Structure, regulation and evolution of Nox-family NADPH oxidases that produce reactive oxygen species, FEBS J. 275 (2008) 3249–3277.
[2] Y. Groemping, K. Rittinger, Activation and assembly of the NADPH oxidase: a structural perspective, Biochem. J. 386 (2005) 401–416.
[3] M.T. Quinn, K.A. Gauss, Structure and regulation of the neutrophil respiratory burst oxidase: comparison with nonphagocyte oxidases, J. Leukoc. Biol. 76 (2004) 760–781.
[4] A. Fuchs, M.C. Dagher, J. Faure, P.V. Vignais, Topological organization of the cytosolic activating complex of the superoxide-generating NADPH-oxidase. Pinpointing the sites of interaction between p47phoz, p67phox and p40phox using the two-hybrid system, Biochim. Biophys. Acta 1312 (1996) 39–47.
[5] K. Lapouge, S.J. Smith, Y. Groemping, K. Rittinger, Architecture of the p40–p47–p67phox complex in the resting state of the NADPH oxidase. A central role for p67phox, J. Biol. Chem. 277 (2002) 10121–10128.
[6] F.B. Wientjes, G. Panayotou, E. Reeves, A.W. Segal, Interactions between cytosolic components of the NADPH oxidase: p40phox interacts with both p67phox and p47phox, Biochem. J. 317 (Pt 3) (1996) 919–924.
[7] P.G. Heyworth, J.T. Curnutte, W.M. Nauseef, B.D. Volpp, D.W. Pearson, H. Rosen, R.A. Clark, Neutrophil nicotinamide adenine dinucleotide phosphate oxidase assembly. Translocation of p47-phox and p67-phox requires interaction between p47-phox and cytochrome b558, J. Clin. Invest. 87 (1991) 352–356.
[8] S. Dusi, M. Donini, F. Rossi, Mechanisms of NADPH oxidase activation: translocation of p40phox, Rac1 and Rac2 from the cytosol to the membranes in human neutrophils lacking p47phox or p67phox, Biochem. J. 314 (Pt 2) (1996) 409–412.
[9] F.R. Sheppard, M.R. Kelher, E.E. Moore, N.J. McLaughlin, A. Banerjee, C.C. Silliman, Structural organization of the neutrophil NADPH oxidase: phosphorylation and translocation during priming and activation, J. Leukoc. Biol. 78 (2005) 1025–1042.
[10] P.G. Heyworth, B.P. Bohl, G.M. Bokoch, J.T. Curnutte, Rac translocates independently of the neutrophil NADPH oxidase components p47phox and p67phox. Evidence for its interaction with flavocytochrome b558, J. Biol. Chem. 269 (1994) 30749–30752.
[11] Y. Gorzalczany, N. Sigal, M. Itan, O. Lotan, E. Pick, Targeting of Rac1 to the phagocyte membrane is sufficient for the induction of NADPH oxidase assembly, J. Biol. Chem. 275 (2000) 40073–40081.
[12] A. Shiose, H. Sumimoto, Arachidonic acid and phosphorylation synergistically induce a conformational change of p47phox to activate the phagocyte NADPH oxidase, J. Biol. Chem. 275 (2000) 13793–13801.
[13] K. Hata, T. Ito, K. Takeshige, H. Sumimoto, Anionic amphiphile-independent activation of the phagocyte NADPH oxidase in a cell-free system by p47phox and p67phox, both in C terminally truncated forms. Implication for regulatory Src homology 3 domain-mediated interactions, J. Biol. Chem. 273 (1998) 4232–4236.
[14] Y. Groemping, K. Lapouge, S.J. Smerdon, K. Rittinger, Molecular basis of phosphorylation-induced activation of the NADPH oxidase, Cell 113 (2003) 343–355.
[15] J. Marcoux, P. Man, M. Castellan, C. Vives, E. Forest, F. Fieschi, Conformational changes in p47(phox) upon activation highlighted by mass spectrometry coupled to hydrogen/deuterium exchange and limited proteolysis, FEBS Lett. 583 (2009) 835–840.
[16] Dang, P.M. et al. The NADPH oxidase cytosolic component p67phox is constitutively phosphorylated in human neutrophils: Regulation by a protein tyrosine kinase, MEK1/2 and phosphatases 1/2A. Biochem Pharmacol 82, 1145–52.
[17] M.C. Faure, et al., The recruitment of p47(phox) and Rac2G12V at the phagosome is transient and phosphatidylserine dependent, Biol. Cell. 105 (2013) 501–518.
[18] Tlili, A., Erard, M., Faure, M.C., Baudin, X., Piolot, T., Dupre-Crochet, S. and Nusse, O. Stable accumulation of p67phox at the phagosomal membrane and ROS production within the phagosome. J Leukoc Biol 91, 83–95.
[19] K. Miyano, H. Fukuda, K. Ebisu, M. Tamura, Remarkable stabilization of neutrophil NADPH oxidase using RacQ61L and a p67phox–p47phox fusion protein, Biochemistry 42 (2003) 184–190.
[20] J. Marcoux, P. Man, I. Petit-Haertlein, C. Vives, E. Forest, F. Fieschi, p47phox molecular activation for assembly of the neutrophil NADPH oxidase complex, J. Biol. Chem. 285 (2010) 28980–28990.
[21] L. Baciou, M. Erard, M.C. Dagher, T. Bizouarn, The cytosolic subunit p67phox of the NADPH-oxidase complex does not bind NADPH, FEBS Lett. 583 (2009) 3225–3229.
[22] T. Akasaki, H. Koga, H. Sumimoto, Phosphoinositide 3-kinase-dependent and -independent activation of the small GTPase Rac2 in human neutrophils, J. Biol. Chem. 274 (1999) 18055–18059.
[23] S.S. Iyer, D.W. Pearson, W.M. Nauseef, R.A. Clark, Evidence for a readily dissociable complex of p47phox and p67phox in cytosol of unstimulated human neutrophils, J. Biol. Chem. 269 (1994) 22405–22411.
[24] T.L. Leto, A.G. Adams, I. de Mendez, Assembly of the phagocyte NADPH oxidase: binding of Src homology 3 domains to proline-rich targets, Proc. Natl. Acad. Sci. U. S. A. 91 (1994) 10650–10654.
[25] L.C. McPhail, SH3-dependent assembly of the phagocyte NADPH oxidase, J. Exp. Med. 180 (1994) 2011–2015.
[26] B.M. Babior, R. Kuver, J.T. Curnutte, Kinetics of activation of the respiratory burst oxidase in a fully soluble system from human neutrophils, J. Biol. Chem. 263 (1988) 1713–1718.
[27] M.A. Ostuni, M. Gelinotte, T. Bizouarn, L. Baciou, C. Houee-Levin, Targeting NADPH-oxidase by reactive oxygen species reveals an initial sensitive step in the assembly process, Free Radic. Biol. Med. 49 (2010) 900–907.
[28] D.J. Uhlinger, K.L. Taylor, J.D. Lambeth, p67-phox enhances the binding of p47-phox to the human neutrophil respiratory burst oxidase complex, J. Biol. Chem. 269 (1994) 22095–22098.
[29] A.R. Cross, R.W. Erickson, J.T. Curnutte, The mechanism of activation of NADPH oxidase in the cell-free system: the activation process is primarily catalytic and not through the formation of a stoichiometric complex, Biochem. J. 341 (Pt 2) (1999) 251–255.
[30] J.L. Freeman, J.D. Lambeth, NADPH oxidase activity is independent of p47phox in vitro, J. Biol. Chem. 271 (1996) 22578–22582.
[31] Y. Maehara, K. Miyano, S. Yuzawa, R. Akimoto, R. Takeya, H. Sumimoto, A conserved region between the TPR and activation domains of p67phox participates in activation of the phagocyte NADPH oxidase, J. Biol. Chem. 285 (2010) 31435–31445.
[32] V. Koshkin, O. Lotan, E. Pick, The cytosolic component p47(phox) is not a sine qua non participant in the activation of NADPH oxidase but is required for optimal superoxide production, J. Biol. Chem. 271 (1996) 30326–30329.
[33] A. Toporik, Y. Gorzalczany, M. Hirshberg, E. Pick, O. Lotan, Mutational analysis of novel effector domains in Rac1 involved in the activation of nicotinamide adenine dinucleotide phosphate (reduced) oxidase, Biochemistry 37 (1998) 7147–7156.
[34] M.H. Paclet, A.W. Coleman, S. Vergnaud, F. Morel, P67-phox-mediated NADPH oxidase assembly: imaging of cytochrome b558 liposomes by atomic force microscopy, Biochemistry 39 (2000) 9302–9310.
[35] X.J. Li, W. Tian, N.D. Stull, S. Grinstein, S. Atkinson, M.C. Dinauer, A fluorescently tagged C-terminal fragment of p47phox detects NADPH oxidase dynamics during phagocytosis, Mol. Biol. Cell 20 (2009) 1520–1532.
[36] J.T. Curnutte, R.W. Erickson, J. Ding, J.A. Badwey, Reciprocal interactions between protein kinase C and components of the NADPH oxidase complex may regulate superoxide production by neutrophils stimulated with a phorbol ester, J. Biol. Chem. 269 (1994) 10813–10819.
[37] T. Yeung, et al., Contribution of phosphatidylserine to membrane surface charge and protein targeting during phagosome maturation, J. Cell Biol. 185 (2009) 917–928.
[38] J.D. Matute, et al., A new genetic subgroup of chronic granulomatous disease with autosomal recessive mutations in p40 phox and selective defects in neutrophil NADPH oxidase activity, Blood 114 (2009) 3309–3315.
[39] D. Diekmann, A. Abo, C. Johnston, A.W. Segal, A. Hall, Interaction of Rac with p67phox and regulation of phagocytic NADPH oxidase activity, Science 265 (1994) 531–533.
[40] H. Koga, H. Terasawa, H. Nunoi, K. Takeshige, F. Inagaki, H. Sumimoto, Tetratricopeptide repeat (TPR) motifs of p67(phox) participate in interaction with the small GTPase Rac and activation of the phagocyte NADPH oxidase, J. Biol. Chem. 274 (1999) 25051–25060.